AIP | Journal of Applied Physics

Effect of Si-induced defects on 1μm absorption losses in laser-grade YAG ceramics

R. Gaume, Y. He, A. Markosyan, and R. L. Byer

Citation: J. Appl. Phys. **111**, 093104 (2012); doi: 10.1063/1.4709756
View online: http://dx.doi.org/10.1063/1.4709756
View Table of Contents: http://jap.aip.org/resource/1/JAPIAU/v111/i9
Published by the AIP Publishing LLC.

Effect of Si-induced defects on 1 μm absorption losses in laser-grade YAG ceramics

R. Gaume,[1,2,a)] Y. He,[2] A. Markosyan,[2] and R. L. Byer[2]
[1]*University of Central Florida, CREOL, 4000 Central Florida Boulevard, Orlando, Florida 32816, USA*
[2]*Edward L. Ginzton Laboratory, 348 Via Pueblo Mall, Stanford University, California 94305, USA*

(Received 28 February 2012; accepted 30 March 2012; published online 3 May 2012)

High sensitivity optical absorption at 1 μm was measured in 40 undoped and Nd-doped $Y_3Al_5O_{12}$ (YAG) transparent ceramics and single crystals using photothermal common-path interferometry. Concurrently, chemical trace analysis was performed on those samples by glow discharge mass-spectroscopy. Silicon and calcium were found to be the major impurities with concentrations up to 250 wt. ppm. A univocal linear correlation between the Si content and the absorption loss at 1 μm is revealed and a possible mechanism for the formation of Si-induced color centers based on a bound polaron model is discussed. Solutions to reduce this optical absorption in ceramics are also proposed. © *2012 American Institute of Physics*. [http://dx.doi.org/10.1063/1.4709756]

I. INTRODUCTION

Ceramic-based gain media offer several advantages over their single-crystalline counterparts in laser applications requiring very high powers, good beam quality, and large apertures.[1–4] Such potential has recently been demonstrated in a 100 kW-class laser using diode pumped 10×10 cm Nd:YAG ceramic slabs with near 20% efficiency and high beam quality.[5,6] These high power applications place stringent demands on the ceramic fabrication process to keep the host absorption levels to a minimum and prevent heating and photo-induced damage by solarization or photodarkening.[7,8] Numerous studies have been devoted to the characterization of optical absorption bands in YAG single crystals and ceramics, which revealed their interdependence with the phonon spectrum of the host lattice[9–11] and various point defects such as cation impurities (e.g., Fe (Refs. 12 and 23) and Mn (Refs. 13 and 14)), hydroxyl groups,[15] and oxygen vacancies.[16,17] The corresponding color center bleaching methods such as air annealing for transition ions and reactively atmosphere processing for hydroxyl groups were proposed and validated, while other intrinsic defects still remain. The intentional use of aliovalent Si doping, up 0.2 mol. %, as a sintering aid for the fabrication of YAG transparent ceramics has, therefore, raised concerns on its potentially deleterious effect on the host absorption. While in a recent study, Stevenson *et al.*[18] did not observe any Si-induced color centers using spectrophotometry, Yagi *et al.*[19] hypothesized that Si-induced charge compensation was the cause of ceramic solarization observed under flash-lamp pumping.

In this paper, we describe the use of photothermal common-path interferometry (PCI),[20–23] a highly sensitive technique, to measure absorption levels as low as several ppm/cm at 1 μm in transparent ceramics and single crystals of YAG and to investigate a possible correlation between the presence of chemical impurities and their absorption properties.

II. EXPERIMENTS

In this work, highly sensitive 1 μm absorption losses are measured by (PCI). This technique optically probes a modulated thermal lensing produced by a 3 W Nd:YAG laser, emitting at 1 μm, and being focused down to a 40 μm-spot in the bulk of a sample.[22,23] The sensitivity, spatial resolution, and linearity of this technique are determined by the proper choice of pump power and spot size. Sensitivities on the order of 1 ppm/cm surpass the typical performance of standard spectrophotometers by 4 orders of magnitude, and highly localized measurements enable 3D absorption mapping within the entire sample volume. By monitoring the phase lag between the pump and the probe signal, the absorption measurement can also be made independent of scattering in samples containing small numbers of scattering centers. Complementary absorption studies between 200 nm and 2 μm have been carried out with a Cary 500i UV-Vis spectrophotometer (Varian, Inc., CA). Chemical trace analysis on 27 potential impurity elements (Na, Mg, Si, P, K, Ga, V, Cr, Mn, Fe, Co, Ni, Cu, Sr, Ce, Pr, Nd, Sm, Eu, Gd, Tb, Dy, Ho, Er, Tm, Yb, Lu) was conducted by glow-discharge mass-spectroscopy (GDMS) with detection limits down to the ppb level (Evans Analytical Group, NY).

III. SAMPLE PREPARATION

The 20 undoped and 1 at. % Nd doped cm-size transparent YAG ceramic samples used in this study were either obtained from commercial sources including Konoshima chemical Co. Ltd., World Lab. Co. Ltd., and Covalent Materials Co. or fabricated in our laboratory following a fabrication process described in Ref. 1. All ceramic samples were either prepared by sintering of YAG nanopowders (non-reactively sintered ceramics, C_{NRS}) or by sintering of stoichiometric mixtures of Y_2O_3 and Al_2O_3 powders (reactively sintered ceramics, C_{RS}).

For comparison purposes, another 20 undoped and Nd-doped YAG single crystals obtained from Scientific Materials Co., Northrop Grumman Synoptics, and Saint-Gobain Co. were also added to this study.

[a)]Electronic mail: gaume@ucf.edu.

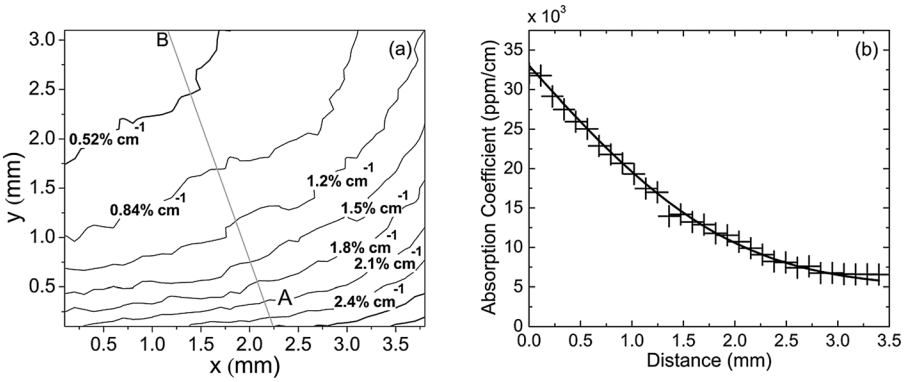

FIG. 1. (a) Two-dimensional absorption coefficient mapping profile (3 × 3.5 mm) of one YAG ceramic sample with a 100 μm spatial resolution before annealing. (b) The absorption coefficient variation from position A to B with steepest gradient in (a) is fitted with error function. The fitted diffusion length is 2.2 mm corresponding to the combined grain boundary and bulk diffusivity of oxygen in the order of 10^{-7} cm^2/s.[24]

Because the conditions used for the sintering of ceramics and the growth of single-crystals lead to oxygen-deficient YAG, absorption levels and absorption profiles are highly sample-dependent and inhomogeneous within the sample volumes. As an example, Fig. 1(a) shows the typical absorption profile of a ceramic sample measured by PCI before annealing. The local absorption coefficient varies, on a centimeter scale, between 1000 and 10 000 ppm/cm, following a pattern consistent with the diffusion of oxygen vacancies (Fig. 1(b)). The optical absorption homogenizes after air-annealing at 1200°C for 5 days, under which conditions are sufficient to in-diffuse oxygen fully in cm-size samples.[14] The optical absorption drops below the detection limit of most spectrophotometers[18] and equilibrates at values ranging from a few ppm/cm to a couple of thousands ppm/cm depending on the sample. For the sake of our investigation and to allow for sample-to-sample comparisons, all samples measured in this work were heat-treated at 1200°C for 5 days.

IV. RESULTS AND DISCUSSIONS

Figure 2 shows the thermalized absorption coefficients at 1 μm of undoped and Nd doped YAG ceramics and single crystals measured by the PCI technique. The absorption coefficient of YAG ceramics varies in a range of 100 to 8000 ppm/cm, which is typically one order of magnitude higher than that of YAG single-crystals (SC). In this study, the lowest absorption coefficient measured in ceramics was comparable to that measured in typical YAG single crystals. In the limited set of samples investigated here, it is worth noting that reactively sintered[1] ceramics (C_{RS}), including doped and undoped samples typically have higher thermalized absorption than non-reactively sintered[25] ceramics (C_{NRS}). Figure 3 displays in-line transmittance measurement in ceramics and reveals the presence of multiple weak absorption bands from 1.2 to 3.1 eV. These spectroscopic features have been ascribed to the presence of electrons trapped on oxygen vacancies and stabilized by cation impurities (F_A centers).

Whereas electrons trapped on oxygen vacancy sites (F^+ centers) form a hydrogen-like system, the presence of an impurity in the coordination sphere of the oxygen vacancy favors the formation of a bound-polaron. The energy levels of such a polaron can be modeled by a linear harmonic oscillator, as first shown in Mn:YAG by Bernhardt.[14] Using this interpretation, one can verify, after fitting the absorption bands shown in Fig. 3, that the bands' centroids are separated by a constant energy, $\Delta E = \Delta n \cdot h\nu_o$. Here, 1/2 $h\nu_0$ represents

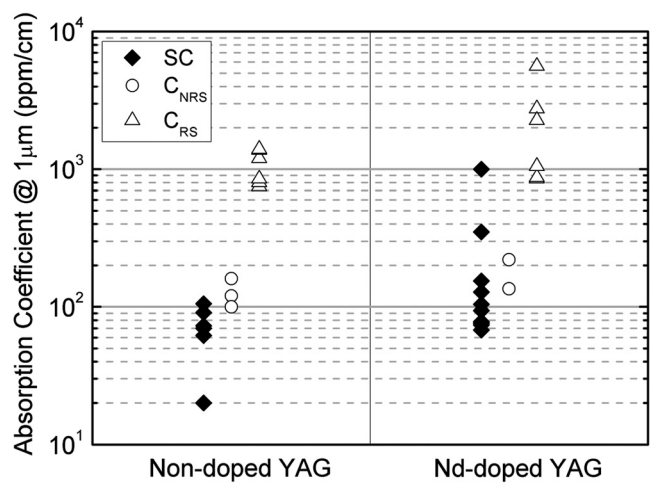

FIG. 2. Absorption coefficient of non-doped YAG (left halves) and Nd-doped YAG (right halves) ceramics and single crystals at 1064 nm. Closed diamonds, open dots, and open triangles represent single crystals (SC), non-reactively sintered ceramics (C_{NRS}), and reactively sintered ceramics (C_{RS}), respectively.

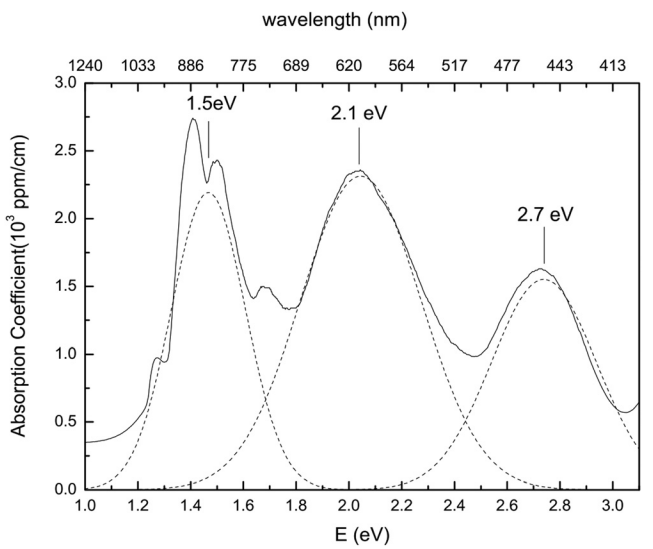

FIG. 3. In-line transmittance measurement from 1.2 to 3.1 eV (1 μm to 400 nm) of a ceramic sample. Blue and red lines represent measured and fitted spectra, respectively. The equally spaced bands 1.5 eV, 2.1 eV, and 2.7 eV are fitted using a bound polaron model.

the zero point energy of the oscillator and Δn the difference in the principal oscillator quantum numbers. Dipolar electric transition selection rules require Δn to be an even integer. The equally spaced absorption bands observed in ceramics and the fitted value 0.6 eV for 2 $h\nu_0$ are consistent with the results of Ref. 14 and confirm the presence of a self-trapped polaron localized near an aliovalent impurity, i.e., whose valences are other than 3+, substituting for Y^{3+} or Al^{3+}.

Typical chemical impurity contents measured by GDMS in YAG single-crystals (SC), non-reactively sintered YAG ceramics (C_{NRS}), and reactively sintered YAG ceramics (C_{NRS}) are listed in Table I. For the sake of conciseness, transition metal elements V, Mn, Co and Ni, and rare-earth ions other than Nd are represented by the acronyms TM and RE, respectively. The concentrations of most trace impurities are below the detection threshold indicated in parentheses.

Similarly to what other investigators have measured,[26,27] we found that Si was the main impurity with concentrations ranging from 1 to 240 wt. ppm. Si concentration in ceramics is typically higher than in single-crystals due to intentional Si-doping, introduced in the form of SiO_2 or tetraethyl orthosilicate to promote ceramic densification.[1] In a separate study, we found that for reactively sintered ceramics, about 60 mol. % of the Si initially introduced had evaporated in the form of SiO_x ($x < 2$) after vacuum sintering at 1750°C for 20 h. For this reason, and contrary to other work,[18] we have chosen to measure the silicon content after sintering. The levels of the other contaminants, such as calcium, transition metal, and rare-earth elements are believed to originate from impure starting powders and cross-contamination during sample preparation. Within the sample set investigated, only three ceramic samples exhibited high levels of silicon and calcium, while the rest of the samples had calcium concentrations below 10 mol. ppm.

Fig. 4 shows that the 1 μm absorption coefficient strongly correlates with the Si concentration. No correlation was found with other trace contaminants such as Cr which were also considered to produce absorption at 1 μm. Given the absorption cross section of Cr^{4+} at 1 μm (5×10^{-18} cm^2)[29] and typical 2% fraction of Cr^{4+} in balance with Cr^{3+} after annealing, the measured Cr content could only count for 1/10 of the total absorption. Si therefore appears as the most likely origin of the observed F_A centers (V_o^+) in this oxidized YAG sample set.

TABLE I. The measured concentration range (in wt. ppm) of impurities in YAG samples, in a descending order of their impurity concentrations.

Impurity	SC	C_{NRS}	C_{RS}
Si	1 to 10	30 to 45	100 to 240
Ca	(<0.5)	0.3 to 3.5	1 to 240
Fe	(<1)	(<1)	2 to 4.2
Cr	(<0.5)	(<0.5)	1 to 2.2
Mg	(<0.1)	(<0.1)	1 to 1.2
Na	0.1 to 0.2	1 to 2.5	1 to 2
Sr	(<0.05)	(<0.05)	0.15 to 0.2
P	(<0.1)	0.5 to 0.8	(<0.1)
K	(<0.5)	(<0.5)	(<0.5)
Cu	(<10)	(<10)	(<10)
TM	(<0.5)	(<0.5)	(<0.5)
RE	(<0.1)	0.1 to 0.5	0.1 to 0.8
Nd[a]	0.2 to 0.4	0.2 to 0.4	3 to 4

[a]Nd concentration measured in undoped YAG samples.

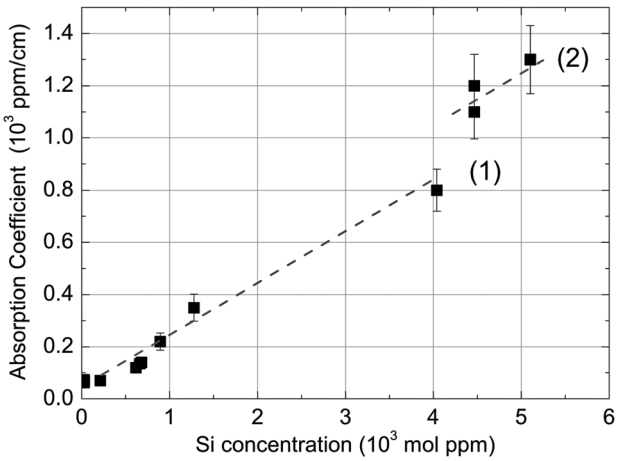

FIG. 4. Dependence of 1 μm absorption coefficient of different YAG samples on their Si impurity concentration for (1) Ca concentration [Ca] < 0.5 wt. ppm and (2) [Ca] = 240 wt. ppm. The dashed line is added for visualization purposes.

It is worth considering the interdependence of Si content and 1 μm absorption in two sample subsets: (1) one in which the calcium concentration in each sample is at detection limits: [Ca] ≪ [Si] and (2) a second in which the calcium concentration is large and constant (240 wt. ppm) and comparable to the silicon concentration: [Ca] ~ [Si]. In the former case, a linear relation between the absorption, α, and the concentration of Si is observed in the range of 100 to 4000 mol. ppm

$$\alpha = k_{Si} \cdot [Si] + \alpha_{0,} \quad (1)$$

where k_{Si} is the fitted empirical constant. An extrapolation of the trend observed in Fig. 4 suggests that, at low Si concentrations, the absorption in ceramics and single crystals does not vanish and reaches a minimum value α_0 of about 50 ppm/cm, controlled by the overall extrinsic and intrinsic defects. For the Ca- and Si-rich ceramic samples, a similar linear dependence with a positive offset, Δα, is drawn: $\alpha = k_{Si} \cdot [Si] + \Delta\alpha + \alpha_0$. The increased absorption level can only be explained by an independent contribution of dilute Si and Ca, since charge compensation between these two ions when neighboring[36] would create fewer color centers and therefore decrease absorption. Because of identical Ca concentration levels in the Ca-rich samples subset, the value $\Delta\alpha = k_{Ca} \cdot [Ca]$ is constant within this lot and the trend given by Eq. (1) is preserved. In fact, color centers associated with Ca impurities have been shown to produce absorption bands in the near UV that tail off around 700 nm.[28] Based on these findings, only a limited absorption caused by Ca-induced color centers might indeed extend into the 1 μm region.

Kuklja *et al.*[30] however showed that, contrary to the case with monovalent and divalent impurities (Eq. (2)), the energetics of Si^{4+}-induced point defects in YAG do not favor the formation of oxygen vacancies

$$MO + Y_Y^x \leftrightarrow M_Y^{'} + \frac{1}{2}V_O^{\cdot\cdot} + \frac{1}{2}Y_2O_3, \quad (2)$$

$$SiO_2 + Al_{Al}^x + \frac{1}{3}Y_Y^x \leftrightarrow Si_{Al}^{\cdot} + \frac{1}{3}V_Y^{'''} + \frac{1}{3}YAlO_3 + \frac{1}{3}Al_2O_3. \quad (3)$$

In a separate work by Fagundes *et al.*,[31] oxygen vacancies were found to charge-compensate divalent Si^{2+} in reduced Si:YAG. To explain the occurrence of color centers in our samples and the trend shown in Fig. 4, we propose that oxygen vacancies induced by divalent Si^{2+} remain in the samples even after long air-annealing at 1200°C. The small Si^{4+} ions (0.41 Å) are thought to occupy the tetrahedral sites of the YAG lattice, whereas the larger Si^{2+} ions (0.9 Å)[32] are presumed to occupy the octahedral Al sites. Thus, the incorporation of Si would not only rely on a redox mechanism but also on a Si site exchange as expressed by the equilibrium

$$Si_{Al(t)}^{\cdot} + Al_{Al(o)}^x + O_o^x \leftrightarrow Si_{Al(o)}^{'} + V_o^{\cdot\cdot} + Al_{Al(t)}^x + \frac{1}{2}O_2 \uparrow, \quad (4)$$

where $Si_{Al(t)}^{\cdot}$ and $Si_{Al(o)}^{'}$ correspond to a tetravalent Si^{4+} and divalent Si^{2+} ion substituting for a tetrahedral and octahedral Al site, respectively. The proximity of the $Si_{Al(o)}^{'}$ defect with the oxygen vacancy $V_o^{\cdot\cdot}$ could favor the formation of a stable cluster complex[30,33]

$$Si_{Al(o)}^{'} + V_o^{\cdot\cdot} \rightarrow [Si_{Al(o)}^{'} \cdots V_o^{\cdot\cdot}]^{'}, \quad (5)$$

which can be modeled by a bound polaron as described earlier. Therefore, the equilibrium constant of Eq. (4) is thought to involve the concentration of the F_A centers $[Si_{Al(o)}^{'} \cdots V_o^{\cdot\cdot}]^{'}$

$$K_F = \frac{[F_A]P_{O_2}^{1/2}[Al_{Al(t)}^x]}{[Si_{Al(t)}][Al_{Al(o)}^x][O_O^x]} \sim \frac{[F_A]PO_{O_2}^{1/2}}{[Si^{4+}]}. \quad (6)$$

Assuming that, under the air-annealing conditions chosen in this experiments, the Si^{2+} concentration is negligible compared to the Si^{4+} concentration: $[Si^{4+}] \gg [Si^{2+}] = [F_A]$, the $[Si^{4+}]$ concentration can be approximated by the total amount of Si. Equation (6) can be simplified to

$$[F_A] \sim K_F[Si]P_{O_2}^{-1/2}, \quad (7)$$

which predicts a linear relationship between the optical absorption and the Si impurity content of the material. The previous assumption $[Si^{4+}] \gg [Si^{2+}]$ has been tested on all the samples investigated in this work by comparing the measured Si content to the concentration of color centers obtained from the Smakula formula[34,35]

$$[F_A] = 0.87 \times 10^{17} KW\left(\frac{n}{n^2+2}\right)\Big/ f_0. \quad (8)$$

In this formula, K and W are the respective maximum and FWHM of the polaron absorption band, and n and f_0 are the material refractive index and oscillator strength for the corresponding absorption transition. The highest F_A center concentration obtained through this method is on the order of $10^{13}\,cm^{-3}$, that is 6 orders of magnitude smaller than the total Si concentration.

Finally, Le Chateliers' principle applied to Eq. (4) suggests that lower concentrations of Si^{2+} can be achieved by using higher oxygen partial pressures and lower annealing temperatures. Thus, to minimize absorption at 1 μm, the annealing temperature should be reasonably adjusted to balance the effect between low concentrations of Si^{2+} and removal of pre-existing oxygen vacancies.

V. CONCLUSION

The presence of impurities in laser materials often leads to undesired absorption bands, which degrades laser efficiency. A fundamental understanding of the origins of these defects is essential for laser materials development and power scaling. In this work, we have specifically investigated the relationship between the impurity content and absorption at the 1 μm emission wavelength of Nd:YAG in 40 undoped and Nd-doped YAG ceramics and single crystals. The broad nature and origins of the samples provided for a wide range of Si and Ca impurity concentrations (0.5 to 200 ppm wt.) as well as widely spread absorption levels (20 to 8000 ppm/cm). The absorption coefficient at 1 μm was found to scale linearly with the Si content. Additional absorption spectroscopy confirmed that Si impurities stabilize electrons near oxygen vacancies and form bound polarons. We propose that, under typical air annealing conditions, the presence of stable divalent Si^{2+}, in equilibrium with its tetravalent form, is responsible for the formation of F_A color centers and leads to bulk absorption in the near infrared. Our present understanding suggests that this equilibrium will shift towards the formation of decreased amounts of Si^{2+} at high oxygen partial pressures and reasonable low annealing temperatures. Alternative approaches to lowering the absorption coefficient will seek to minimize the amount of Si introduced as a sintering aid in transparent polycrystalline YAG for laser application at 1 μm or to consider the use of isovalent additives such as boron. In either case, additional work will still be necessary to validate this proposed mechanism on both experimental and defect-modeling grounds.

ACKNOWLEDGMENTS

The authors wish to thank Dr. A. Ikesue, Dr. Y. Yanase from Covalent Materials Co. and Northrop Grumman Synoptics Co. for graciously providing some of the samples for this study. This research is supported by the Air Force Office of Scientific Research (AFOSR), Grant No. FA 9550-07-1-0392.

[1]A. Ikesue, T. Kinoshita, and K. Kamata, J. Am. Ceram. Soc. **78**, 1033 (1995).
[2]A. Ikesue, Y. L. Aung, T. Taira, T. Kamimura, K. Yoshida, and G. L. Messing, Annu. Rev. Mater. Sci. **36**, 397 (2006).
[3]A. Ikesue and Y. L. Aung, J. Am. Ceram. Soc. **89**, 1936–1944 (2006).
[4]J. Wisdom, M. Digonnet, and R. L. Byer, Photonics Spectra **38**, 2–8 (2004).
[5]S. J. McNaught, H. Komine, S. B. Weiss, R. Simpson, A. M. F. Johnson, J. Machan, C. P. Asman, M. Weber, G. C. Jones, M. M. Valley, A. Jankevics, D. Burchman, M. McClellan, J. Sollee, J. Marmo, and H. Injeyan,

in 2009 Conference on Lasers and Electro-Optics and Quantum Electronics and Laser Science Conference (CLEO/QELS 2009) (IEEE, 2009).
[6]R. M. Yamamoto *et al*., in Proceedings of the Eighth Annual Directed Energy Symposium, Lihue, HI, November 2005.
[7]H. Yagi, T. Yanagitani, H. Yoshida, M. Nakatsuka, and K. Ueda, Opt. Laser Technol. **39**(6), 1295 (2007).
[8]A. Vaddigiri, K. Simmons-Potter, W. J. Thomes, and D. C. Meister, IEEE Nucl. Plasma Sci. Soc. **53**(6), 3882 (2006).
[9]M. Bass and A. F. Paladino, J. Appl. Phys. **38**, 2706 (1967).
[10]G. A. Slack, D. W. Oliver, R. M. Chrenko, and S. Roberts, Phys. Rev. **177**, 1308 (1969).
[11]E. V. Zharikov, V. I. Zhekov, T. M. Murina, V. V. Osiko, A. M. Prokhorov, and M. I. Timoshechkin, Sov. J. Quantum Electron. **6**(3), 796 (1976).
[12]S. R. Rotman, C. Warde, H. L. Tuller, and J. Haggerty, J. Appl. Phys. **66**, 3207 (1989).
[13]H. J. Bernhart, Phys. Status Solidi A **37**, 445 (1976).
[14]H. J. Bernhart, Phys. Status Solidi B **87**, 213 (1978); H. J. Bernhart, *ibid.* **100**, 117 (1980).
[15]D. P. Devor, R. C. Pastor, and L. G. DeShazer, J. Chem. Phys. **81**(9), 4104 (1984).
[16]J. Chen, T. C. Lu, Y. Xu, A. G. Xu, and D. Q. Chen, J. Phys.: Condens. Matter **20**, 325212 (2008).
[17]K. Mori, Phys. Status Solidi A **42**, 375 (1977).
[18]A. Stevenson, B. Bittel, C. Leh, X. Li, E. Dickey, P. Lenahan, and G. Messing, Appl. Phys. Lett. **98**, 051906 (2011).
[19]H. Yagi, T. Yanagitani, and K.-I. Ueda, J. Alloys Compd. **421**, 95 (2006).
[20]M. E. Long, R. L. Swofford, and A. C. Albrecht, Science **191**, 183 (1976).
[21]W. B. Jackson, N. M. Amer, A. C. Boccara, and D. Fournier, Appl. Opt. **20**, 1333 (1981).
[22]A. Alexandrovski, M. Fejer, A. Markosyan, and R. Route, Proc. SPIE **7193**, 71930D (2009).
[23]A. L. Alexandrovski, R. K. Route, M. M. Fejer, LSC Meeting, Hanfrod WA, 2001, LIGO-GO10352-00Z.
[24]I. Sakaguchi, I. Haneda, H. Tanaka, J. Yanagitani, and T. Yanagitani, J. Am. Ceram. Soc. **79**(6), 1627 (1996).
[25]J. Lu, K.-I., Ueda, H. Yagi *et al*., J. Alloys Compd. **341**, 220 (2002).
[26]J. Huie and R. Gentilman, "Window and dome technologies and materials IX," Proc. SPIE **5786**, 251 (2005).
[27]M. Innocenzi, F. Swimm, M. Bass, R. H. French, and M. R. Kokta, J. Appl. Phys. **68**(3) 1200 (1990).
[28]B. Tissue, M. Jia, W. Lu, L. Yen, and M. William, J. Appl. Phys. **70**(7), 3775 (1991).
[29]H. Eilers, K. R. Hoffman, W. M. Dennis, S. M. Jacobsen, and W. M. Yen, Appl. Phys. Lett. **61**, 2958 (1992).
[30]M. M. Kuklja, J. Phys.: Condens. Matter **12**, 2953 (2000).
[31]D. Fagundes-Peters, N. Martynyuk *et al*., J. Lumin. **125**, 238 (2007).
[32]V. G. Tsirel'son, Yu. Z. Nozik, and V. S. Urusov, Russ. Chem. Rev. **55**(4), 608 (1986).
[33]L. Schuh, R. Metselaar, and C. R. A. Catlow, J. Eur. Ceram. Soc. **7**(2), 67 (1991).
[34]D. L. Dexter, Phys. Rev. **101**, 48 (1956).
[35]Y. Dong, G. Zhou, J. Xu *et al*., J. Cryst. Growth **286**(2), 476 (2006).
[36]Y. Kuru, E. O. Savasir, S. Z. Nergiz, C. Oncel, and M. A. Gulgun, Phys. Status Solidi C **5**(10), 3383 (2008).